# Indirect effects mediate direct effects of climate warming on insect disturbance regimes of temperate broadleaf forests in the central U.S.

## Supplementary Materials

### Appendix S1. Modeling the vegetation dynamics

We used the LANDIS PRO Succession module to simulate vegetation dynamics. Specifically, we used the LINKAGES 3.0 ecosystem process model (Dijak et al., 2017) to estimate species establishment probability (SEP) and maximum growing space (MGSO) for each land type under different climate change scenarios. Land types are landform units that stratify the heterogenous landscape. We used the SEPs and the MGSOs estimated by LINKAGES 3.0 as model parameters in LANDIS PRO to encapsulate the effects of climate change on vegetation (Fig. 2; Wang et al., 2014; Dijak et al., 2017). In LANDIS PRO, SEP together with species shade tolerance and available growing space determines seedling colonization. Competition is initiated once the MGSO is reached, and competition-caused mortality is simulated by using Yoda's self-thinning theory (Yoda, 1963).

**Appendix S2. Modeling the effects of land type and other types of disturbance on insects**

The susceptibility of a given site can be adjusted to reflect variation in the susceptibility introduced by site environment (e.g., top-ridges and south-facing slopes with low soil moisture increase site susceptibility to insect outbreaks) and recent disturbance (e.g., recent defoliation or fire may weaken the stressed host). We used the original design of biotic disturbance agent (BDA) proposed by Sturtevant et al. (2004) to adjust susceptibility based on land type modifiers (LTMs) and disturbance modifiers (DMs). The values of LTMs and DMs range between -1 and 1 (the operator sign depended on how DMs and LTMs affect the site susceptibility to insect outbreak) and are added to the site susceptibility index *S* of all affected sites. It is assumed that the LTMs are constant in the entire simulation, while the DMs with duration decline linearly since last disturbance as shown in Eq. S1:

$$DM_{dist}(t) = DM_{max,dist} \times \frac{DM_{duration,dist} - t_{dist}}{DM_{duration,dist}} \quad \text{Eq. S1}$$

in which $DM_{max,dist}$ is the maximum modifier for the disturbance (*dist*); $DM_{duration,\ dist}$ is the duration of the disturbance (*dist*), $t_{dist}$ is the time since last disturbance experienced on that site. Disturbances included fire, wind, and other BDA agents. Thus, the site susceptibility index *S* is modified by LTM and the sum of all DMs as Eq. S2:

$$S_m(t) = S(t) + LTM + (DM_{dist1}(t) + DM_{dist2}(t) + \cdots) \quad \text{Eq. S2}$$

**Appendix S3. Modeling insect outbreak probability and mortality**

Biotic disturbance probability (BDP) was calculated as follows:

$$BDP = \alpha \times \left(\frac{S_m + NE \times W}{1 + W}\right) \times \left(\frac{R + V}{4}\right) \quad \text{Eq. S3}$$

in which α is a user-defined calibration parameter; $S_m$ is the modified susceptibility. *NE* is the neighborhood effects calculated from the mean $S_m$ of each cell within a user-defined radius by using one of the three radial distance weighting functions: uniform, linear, and Gaussian. *NE* is calculated for all cells containing host species, *W* is a parameter designed to define the relative importance between $S_m$ and *NE*. *R* is defined as the regional outbreak status ranging from 0 (no outbreak) to 3 (severe outbreak). The severity is estimated based on local outbreak records (Haavik & Stephen 2010). *V* is the population-level voltinism that can influence the outbreak status. *R* and *V* together determine the outbreak status of the entire region. To assess the population development of the temperature-dependent woodborer, we calculated the voltinism—the potential number of generations per year. The voltinism *V* affects the severity of insect disturbance by changing the value of BDP. Specifically, *V* is a function of the climate variable (annual degree day sum>5.5℃) ranging from 0.5 to 1 in the BDP equation. $V = 0.5$ indicates poor condition for red oak borer (ROB) population development and the population consists of semivoltine ROB. $V = 1$ means the population consists of univoltine borers. Most of the time, borer population consist of both semi-and univoltine borers ($0.5 < V < 1$), the majority of the population depend on the microclimate that an individual borer experienced during its larval stage. The *V* was derived from and calibrated with field studies and experts' opinions (Aquino et al., 2008).

Therefore, BDP is an emergent property of forest susceptibility, neighborhood effects, insect population dynamics, and regional outbreak status. ROB disturbance severity is a direct

function of BDP in which BDP<0.33 is slight disturbance; 0.33<BDP<0.67 is moderate disturbance; BDP>0.67 is severe disturbance (Sturtevant et al. 2004). Different disturbance severity causes different cohort mortality, and the mortality probabilities (MPs) of host tree species were derived from empirical field studies (Fan et al. 2008). The mortality at an outbreak site is determined by species' age and host susceptibility classes (Table S1). The susceptibility of each cohort to insect-induced mortality was derived from empirical field studies and experts' opinions (Hay, 1969, 1974; Fan et al., 2008).

Table S1. Host susceptibility classes and mortality probability (MP).

| Species | Susceptibility class 3 age (MP) | Susceptibility class 2 age (MP) | Susceptibility class 1 age (MP) |
|---|---|---|---|
| Black oak | 10 (0.5) | 20 (0.4) | 30 (0.08) |
| Northern red oak | 10 (0.6) | 20 (0.5) | 30 (0.1) |
| Southern red oak | 10 (0.5) | 20 (0.33) | 30 (0.05) |
| White oak | 20 (0.3) | 30 (0.2) | 40 (0.02) |
| Post oak | 20 (0.2) | 30 (0.2) | 40 (0.02) |

## Appendix S4. BDA diagram

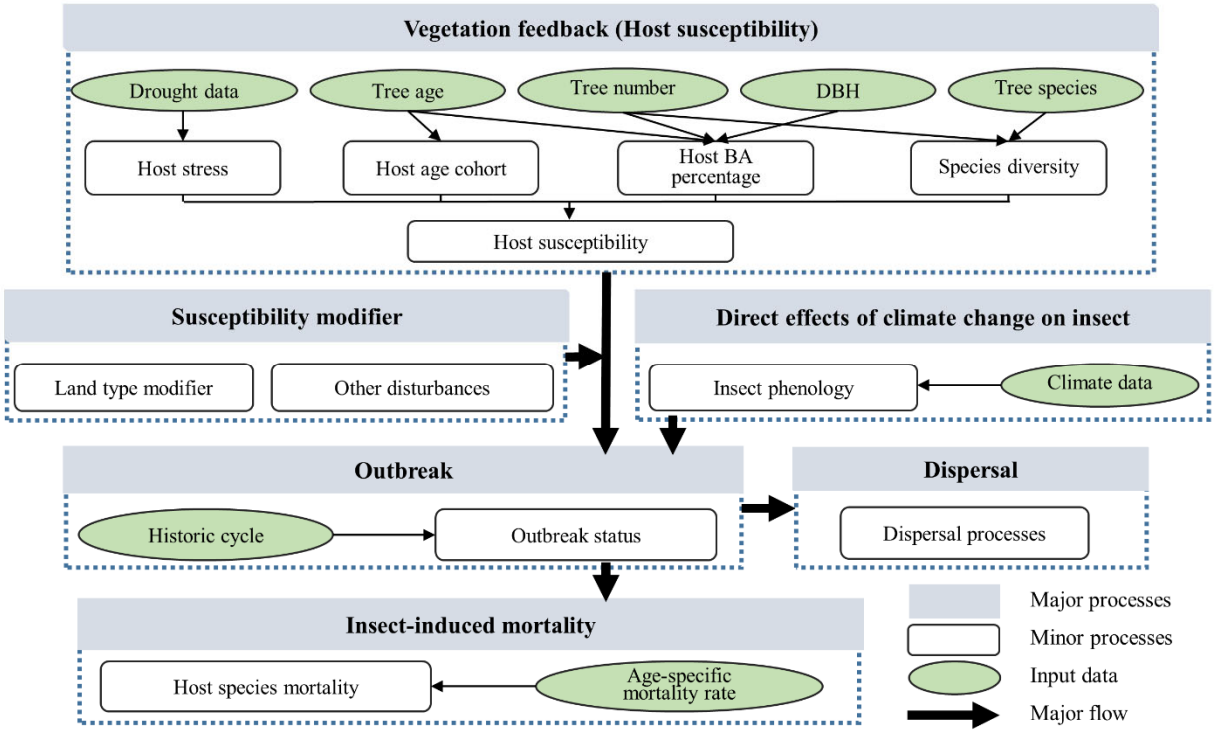


FIGURE. S1 Diagram of the updated BDA module in LANDIS PRO. DBH is tree diameter at breast height (meter), and BA is the basal area ($m^2$/ha).

**Appendix S5. Model parameterization, calibration, and validation**

Species' longevity, maturity, shade tolerance class, seedling dispersal distance, sprouting probability, maximum stand density index, and maximum diameter at breast height (DBH) were parameterized based on previous studies and literature (Burns & Honkala, 1990; Wang et al., 2018) (Table *S* S2, S3, S4). The initial forest composition map in 2000 for the LANDIS PRO was directly derived from 1995-2005 Forest Inventory and Analysis (FIA) data. We used Landscape Builder to stochastically assign a representative FIA plot to each raster cell based on size class, land cover, and landform (Dijak, 2013). Each raster cell on the map contained the initial tree species distribution (absence/presence), abundance (number of trees and DBH by age cohort), and land type (e.g., forest, urban, water body, and agricultural land) (Wang et al., 2014).

The majority of the model calibration was done in previous studies (e.g., Wang et al., 2018, 2019). A data splitting approach was employed to utilize FIA data for both calibration and validation of forest growth and succession (Wang et al., 2014). Discrepancies between model predictions and FIA data at the landscape scale were relatively small: both mean error (ME) and relative root mean square error (RMSE) were less than 10%. Changes in forest basal area, tree density, and quadratic mean diameter in years after simulated harvest were compared with field studies and were in general agreement (Fraser, He, Shifley, Wang, & Thompson 2013). We compared the predicted basal area and tree density from selected raster cells to the observed values in FIA plots and compared the landscape-scale predictions stratified by land type (using 223A Ozark Highlands Section as an example) (Fig. S2 a, b). We compared predicted ROB disturbed area to the dataset of field-based Insect and Disease Detection Survey (IDS) and field studies in Missouri and Arkansas from 2000-2010 to validate the BDA (Fierke et al.,2007; Haavik & Stephen 2010; Fan et al., 2008). Due to the limited temporal and spatial field data of

ROB disturbance, we only compared the simulation values with the observed values in the ecological section or subsection where the data were available. Specifically, we compared the predicted ROB disturbed area (±SD) against observed values of 223Aa St. Francois Knobs and Basins Subsection during 2006-2010, 223Ae Meramec River Hills Subsection during 2006-2010, 223Ad Gasconade River Hills Subsection during 2006-2010, and M223A Boston Mountain Section during 2000-2005 (Fig. S2c).

Table S2 Biological traits of individual tree species and parameters used in the forest dynamic landscape model LANDIS PRO in the central US.

| Spp. common name | Mature/ longevity | Shade tolerance | Fire class | Max dispersal distance (m/year) | Vegetative probability | Min/max sprouting age | Max DBH (cm) | Max SDI (trees/ha) |
|---|---|---|---|---|---|---|---|---|
| Sugar maple | 20/300 | 5 | 5 | 2160 | 0.8 | 20/80 | 75 | 570 |
| Shortleaf pine | 20/200 | 2 | 4 | 1350 | 0.8 | 10/30 | 70 | 990 |
| Loblolly pine | 20/200 | 3 | 4 | 1350 | 0.8 | 10/30 | 70 | 1100 |
| Red maple | 10/150 | 4 | 1 | 2160 | 0.9 | 10/100 | 65 | 700 |
| Mockernut hickory | 30/200 | 3 | 1 | 1080 | 0.6 | 20/200 | 65 | 570 |
| White ash | 30/250 | 3 | 4 | 1620 | 0.6 | 10/150 | 65 | 570 |
| Sweetgum | 30/200 | 2 | 2 | 1620 | 0.6 | 20/200 | 65 | 570 |
| Yellow poplar | 20/200 | 2 | 2 | 2160 | 0.5 | 20/150 | 70 | 700 |
| Black cherry | 20/150 | 2 | 1 | 1080 | 0.8 | 20/100 | 65 | 570 |
| White oak | 40/300 | 4 | 3 | 1080 | 0.7 | 10/100 | 75 | 570 |
| Southern red oak | 30/200 | 3 | 2 | 1080 | 0.7 | 10/100 | 65 | 570 |
| Northern red oak | 30/200 | 3 | 2 | 1080 | 0.7 | 10/120 | 65 | 570 |
| Post oak | 40/250 | 3 | 3 | 1080 | 0.6 | 10/100 | 70 | 570 |
| Black oak | 20/150 | 3 | 2 | 1080 | 0.6 | 10/100 | 65 | 570 |
| American elm | 40/200 | 3 | 2 | 1620 | 0.7 | 10/60 | 60 | 900 |

Species' scientific names are listed in Table S3.

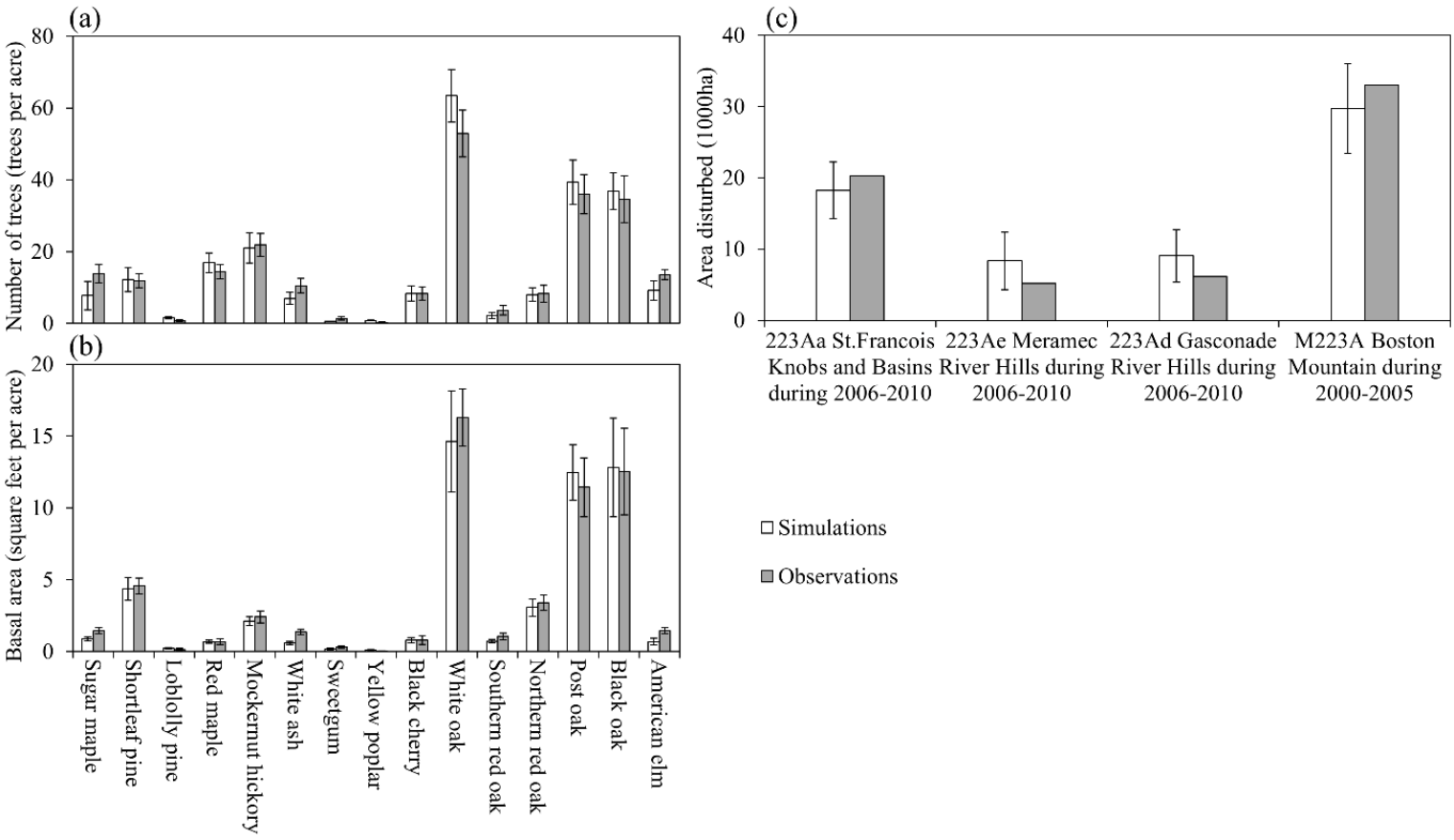


FIGURE. S2 Comparison of the predicted number of trees (a) and basal area (b) by species from the LANDIS PRO model against observed values of 233A Ozark Highlands Section in 2010. Comparison of predicted ROB disturbed area (±SD) against observed values of 223Aa St. Francois Knobs and Basins Subsection during 2006-2010, 223Ae Meramec River Hills Subsection during 2006-2010, 223Ad Gasconade River Hills Subsection during 2006-2010, and M223A Boston Mountain Section during 2000-2005 (c).

**Appendix S6. Temporal changes in mean annual temperature**

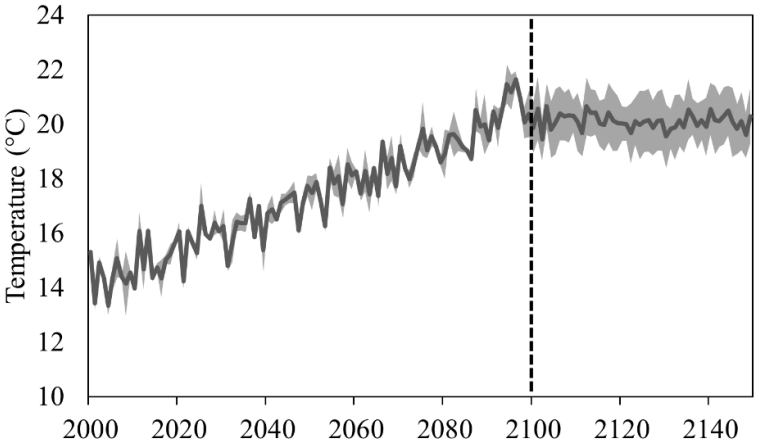


FIGURE. S3 Temporal changes in mean annual temperature under ACCESS1-0 scenario from 2000 to 2099. From 2100 to 2150, the mean annual temperature was randomly sampled from 2080-2099 based on the zero-order approximation that climate will stabilize toward 2150.

**Appendix S7. Sensitivity analysis for the insect model**

We used three general circulation models (GCMs) (ACCESS1.0, CanESM2, and GFDL-ESM2M) in the RCP 8.5 emission scenario used in the IPCC Fifth Assessment Report as climate change scenarios and employed one historic climate observation (1980-2009) as the baseline climate scenario to conduct the sensitivity analysis. Compared to the baseline, the three GCMs projected mean annual temperature in 2070-2100 increased by 5.6℃, 4.8℃, and 3.4℃ respectively. There was a great variation in region-wide precipitation projections among these three GCMs. Precipitation on average decreased 40 mm in ACCESS1-0, and increased 60 and 26 mm in CanESM2 and GFDL-ESM2M, respectively. We set the model stimulating for 300 years from 2000 to 2300 and presented the mean values of voltinism, total susceptibility, and primary host biomass under each climate condition (Fig. S4). The results showed that the predictions of our insect module could capture the variation among different climate scenarios.

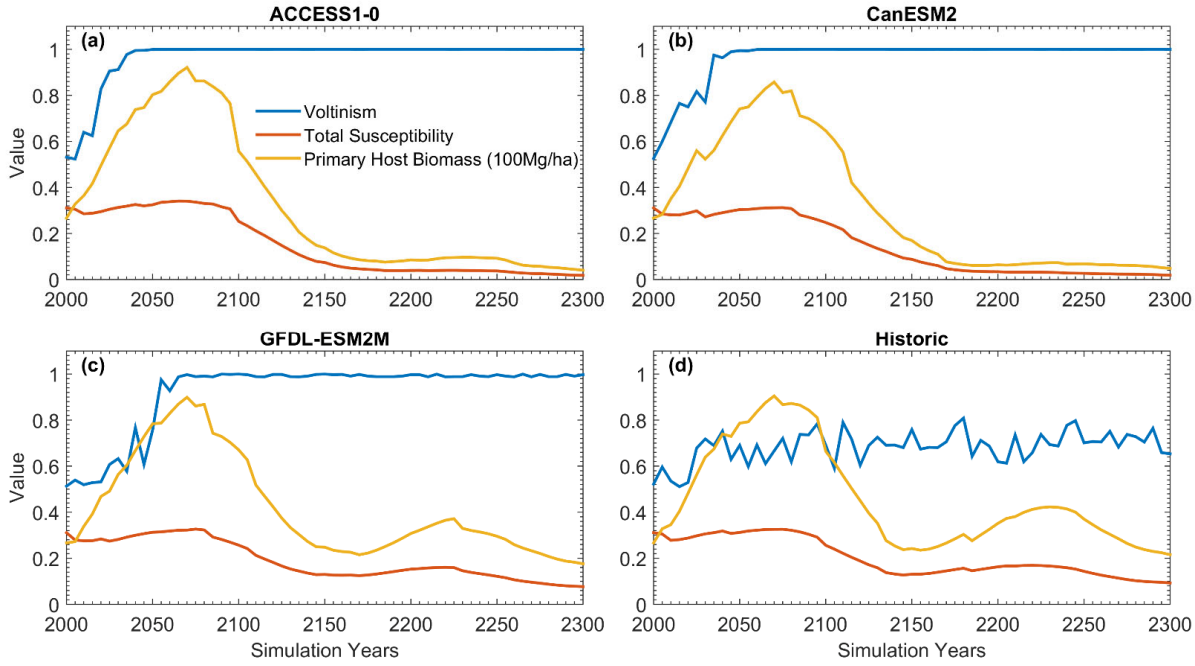


FIGURE. S4 The mean values of voltinism, total susceptibility, and primary host biomass under four climate scenarios from 2000 to 2300 in the Central Hardwood Forests, U.S.

**Appendix S8. Species host type, common name, and scientific name**

Table S3 Species host type, common name, and scientific name

| Host type | Common name | Scientific name |
|---|---|---|
| Non-host | Sugar maple | *Acer saccharum* Marshall |
| Non-host | Red maple | *A.rubrum* L. |
| Non-host | Loblolly pine | *Pinus taeda* L. |
| Non-host | Shortleaf pine | *P. echinata* Mill |
| Non-host | Mockernut hickory | *Carya tomentosa* Nutt. |
| Non-host | White ash | *Fraxinus americana* L. |
| Non-host | Sweetgum | *Liquidambar styraciflua* L. |
| Non-host | Yellow poplar | Liriodendron tulipifera L. |
| Non-host | Black cherry | *Prunus serotina* Ehrh. |
| Secondary host | White oak | *Quercus alba* L. |
| Primary host | Southern red oak | *Q. falcate* Michx |
| Primary host | Northern red oak | *Q. rubra* L. |
| Secondary host | Post oak | *Q. stellate* Wangenh. |
| Primary host | Black oak | *Q. veltutina* Lam |
| Non-host | American elm | *Ulmus americana* L. |

**Appendix S9. Biological traits of individual tree species used in LINKAGES**

Table S4 Biological traits of individual tree species and parameters used in LINKAGES 3.0 in the central U.S. (Drought tolerance: the maximum proportion of growing season that species can withstand drought; Frost tolerance: minimum January temperature species can withstand)

| Spp. Common name | Growing degree days | | Growth parameters | | Drought tolerance | Frost tolerance | Parameters to calculate nitrogen growth factors | | | | | Leaf weight |
|---|---|---|---|---|---|---|---|---|---|---|---|---|
| | maximum | minimum | b3 | b2 | | | cm1 | cm2 | cm3 | cm4 | cm5 | |
| Sugar maple | 3528 | 984 | 0.1272 | 38.17 | 0.08 | -25 | 2.94 | 117.52 | 0.00234 | -1.2 | 1.3 | 440 |
| Shortleaf pine | 5314 | 1892 | 0.2863 | 57.26 | 0.423 | -11 | 2.79 | 219.77 | 0.00179 | -0.6 | 1 | 440 |
| Loblolly pine | 6090 | 2714 | 0.2912 | 58.23 | 0.36 | -6 | 2.79 | 219.77 | 0.00179 | -0.6 | 1 | 440 |
| Red maple | 6891 | 900 | 0.2863 | 57.26 | 0.23 | -25 | 2.79 | 219.77 | 0.00179 | -0.6 | 1 | 440 |
| Mockernut hickory | 5400 | 1900 | 0.2663 | 53.26 | 0.425 | -6 | 2.94 | 120 | 0.002 | -0.9 | 1.2 | 248 |
| White ash | 5866 | 1056 | 0.2863 | 57.26 | 0.28 | -23 | 2.99 | 207.43 | 0.00175 | -5 | 2.9 | 440 |
| Sweetgum | 6142 | 2100 | 0.2152 | 53.81 | 0.3 | -9 | 2.99 | 207.43 | 0.00175 | -5 | 2.9 | 440 |
| Yellow poplar | 6000 | 1588 | 0.1495 | 44.84 | 0.16 | -16 | 2.99 | 207.43 | 0.00175 | -5 | 2.9 | 440 |
| Black cherry | 8258 | 1169 | 0.2863 | 57.26 | 0.3 | -21 | 2.99 | 207.43 | 0.00175 | -5 | 2.9 | 173 |
| White oak | 5314 | 1169 | 0.3363 | 67.26 | 0.33 | -19 | 2.94 | 117.52 | 0.00234 | -1.2 | 1.3 | 440 |
| Southern red oak | 5800 | 2100 | 0.3363 | 67.26 | 0.423 | -9 | 2.94 | 117.52 | 0.00234 | -1.2 | 1.3 | 440 |
| Northern red oak | 4766 | 984 | 0.2863 | 57.26 | 0.225 | -25 | 2.94 | 117.52 | 0.00234 | -1.2 | 1.3 | 440 |
| Post oak | 6142 | 1892 | 0.4201 | 63.01 | 0.555 | -11 | 2.79 | 219.77 | 0.00179 | -0.6 | 1 | 440 |
| Black oak | 5435 | 1437 | 0.2863 | 57.26 | 0.3 | -15 | 2.79 | 219.77 | 0.00179 | -0.6 | 1 | 440 |
| American elm | 2200 | 279 | 0.2912 | 58.23 | 0.401 | -22 | 2.87 | 180 | 0.00207 | -0.9 | 1.2 | 440 |

**Appendix S10. Experimental design**

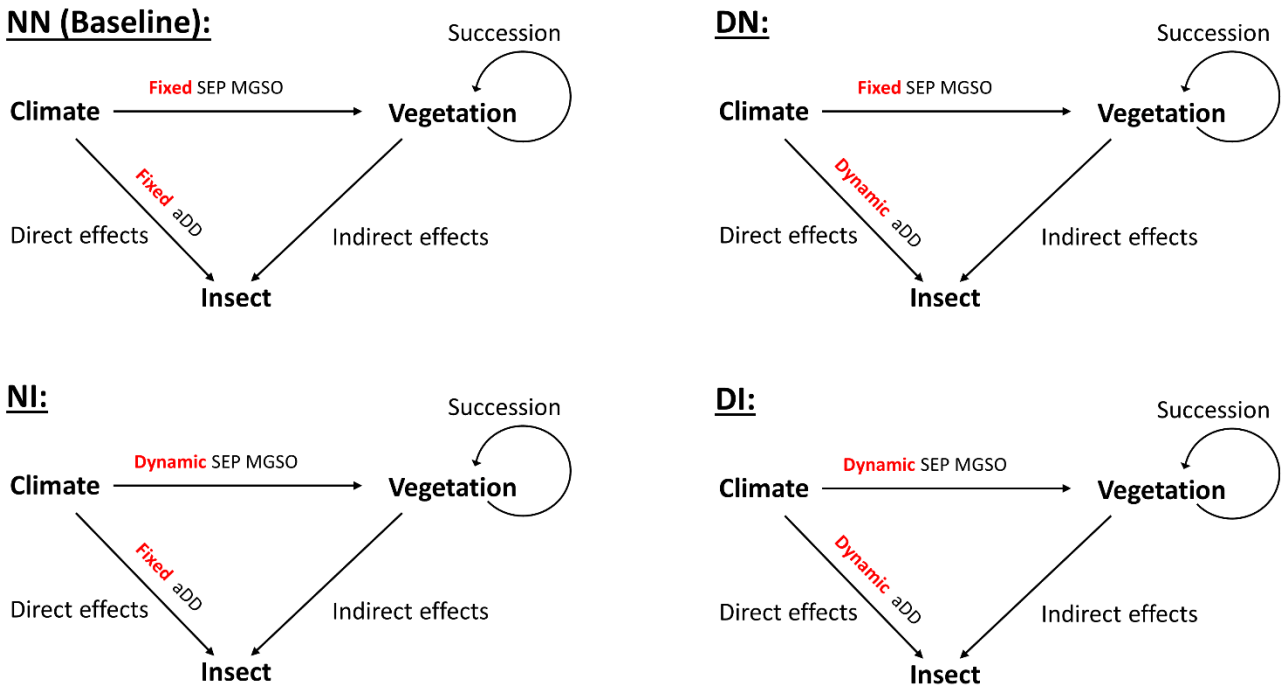


FIGURE. S5 The simulation design for NN, DN, NI, and DI scenarios. Specifically, simulations in the NN scenario were based on baseline climate with fixed forest growth parameters (i.e., SEP and MGSO) and no changes in the direct effects on ROB; simulations in DN scenario in with fixed forest growth parameters while the direct effects on ROB were updated according to RCP 8.5; simulations in the NI scenario included dynamic growth parameters according to RCP 8.5 while no change in the direct effects on ROB and simulations in the DI scenario with both dynamic changes in growth parameters and the direct effects on ROB.

**Appendix S11. Harvest and wildfire**

We simulated the current tree harvest regime with the LANDIS PRO Harvest Module (Fraser et al., 2013). We used US Forest Inventory and Analysis (FIA) units as the management units to capture the variations in harvest practices across the regions by simulating different harvest strategies for each unit. We simulated two types of harvest in each management unit consisting of high-grading and clear-cutting. We varied the percentage of the unit harvested and the preferred species for harvest to capture similar removals to those reported since 1995–2015 (Fraser et al., 2013). Also, we simulated the current natural fire regimes by using the LANDIS PRO Fire Module (Fraser et al., 2019). We did not include any direct effects of climate change on fire regimes in this study. We parameterized the size and frequency of wildfire based on fire records from 1980 to 2014 from LANDFIRE (2012) and Monitoring Trends in Burn Severity (Eidenshink et al., 2007).

**Reference**


Burns, R. M. (1990). *Silvics of North America: Conifers* (No. 654). US Department of Agriculture, Forest Service.

Dijak, W. (2013). Landscape Builder: software for the creation of initial landscapes for LANDIS from FIA data. *Computational Ecology and Software. 3*(2): 17-25.

Eidenshink, J., Schwind, B., Brewer, K., Zhu, Z. L., Quayle, B., & Howard, S. (2007). A project for monitoring trends in burn severity. *Fire ecology*, *3*(1), 3-21. https://doi.org/10.4996/fireecology.0301003

Fan, Z., Kabrick, J. M., Spetich, M. A., Shifley, S. R., & Jensen, R. G. (2008). Oak mortality associated with crown dieback and oak borer attack in the Ozark Highlands. *Forest Ecology and Management*, *255*(7), 2297-2305. https://doi.org 10.1016/j.foreco.2007.12.041

Fierke, M. K., Kelley, M. B., & Stephen, F. M. (2007). Site and stand variables influencing red oak borer, Enaphalodes rufulus (Coleoptera: Cerambycidae), population densities and tree mortality. *Forest Ecology and Management*, *247*(1-3), 227–236. https://doi.org 10.1016/j.foreco.2007.04.051

Fraser, J. S., He, H. S., Shifley, S. R., Wang, W. J., & Thompson III, F. R. (2013). Simulating stand-level harvest prescriptions across landscapes: LANDIS PRO harvest module design. *Canadian Journal of Forest Research*, *43*(10), 972-978. https://doi.org/10.1139/cjfr-2013-0190

Fraser, J. S., Wang, W. J., He, H. S., & Thompson, F. R. III (2019). Modeling post-fire tree mortality using a logistic regress method within a forest landscape model. *Forests*, *10*, 25 doi:10.3390/f10010025

Haavik, L. J., & Stephen, F. M. (2010). Historical dynamics of a native cerambycid, Enaphalodes rufulus, in relation to climate in the Ozark and Ouachita Mountains of Arkansas. *Ecological entomology*, *35*(6), 673-683. https://doi.org 10.1111/j.1365-2311.2010.01225.x

Haavik, L. J., Jones, J. S., Galligan, L. D., Guldin, J. M., & Stephen, F. M. (2012). Oak decline and red oak borer outbreak: impact in upland oak-hickory forests of Arkansas, USA. *Forestry: An International Journal of Forest Research*, *85*(3), 341-352. https://doi.org 10.1093/forestry/cps032

Hay, C. J. (1969). The life history of a red oak borer and its behavior in red, black, and scarlet oak. In *Proceedings. North Central Branch Entomological Society of America* (Vol. 24, No. 2, p. 125127).

Hay, C. J. (1974). Survival and Mortality of Red Oak Borer Larvae1 on Black, Scarlet, and Northern Red Oak2 in Eastern Kentucky. *Annals of the Entomological Society of America*, *67*(6), 981–986. https://doi.org 10.1093/aesa/67.6.981

LANDFIRE. (2012). Vegetation disturbance, LANDFIRE 1.4.0. U.S. Department of the Interior, Geological Survey. Retrieved from http://www.landfire.gov/viewer/

Sturtevant, B. R., Gustafson, E. J., Li, W., & He, H. S. (2004). Modeling biological disturbances in LANDIS: a module description and demonstration using spruce budworm. *Ecological Modelling*, *180*(1), 153-174. https://doi.org 10.1016/j.ecolmodel.2004.01.021

Wang, W. J., He, H. S., Spetich, M. A., Shifley, S. R., Thompson III, F. R., Dijak, W. D., & Wang, Q. (2014). A framework for evaluating forest landscape model predictions using empirical data and knowledge. *Environmental modelling & software*, *62*, 230-239. https://doi.org 10.1016/j.envsoft.2014.09.003

Wang, W. J., Thompson III, F. R., He, H. S., Fraser, J. S., Dijak, W. D., & Spetich, M. A. (2018). Population dynamics has greater effects than climate change on tree species distribution in a temperate forest region. *Journal of biogeography*, *45*(12), 2766-2778. doi:10.1111/jbi.13467

Wang, W. J., Thompson III, F. R., He, H. S., Fraser, J. S., Dijak, W. D., & Jones-Farrand, T. (2019). Climate change and tree harvest interact to affect future tree species distribution changes. *Journal of Ecology*, *107*(4), 1901-1917. doi:10.1111/1365-2745.13144

Yoda, K. (1963). Self‐thinning in overcrowded pure stands under cultivate and natural conditions. Journal of Biology, Osaka City University, 14, 107–129.